Regenerative Therapy 21 (2022) 372–379

Contents lists available at ScienceDirect

Regenerative Therapy

journal homepage: http://www.elsevier.com/locate/reth

Original Article

Rapid and chronological expression of angiogenetic genes is a major mechanism involved in cell sheet transplantation in a rat gastric ulcer model

Shun Yamaguchi [a, #], Miki Higashi [b, #], Kengo Kanetaka [b, *], Yasuhiro Maruya [b], Shinichiro Kobayashi [a], Keiichi Hashiguchi [c], Masaaki Hidaka [a], Kazuhiko Nakao [c], Susumu Eguchi [a]

[a] Department of Surgery, Nagasaki University Graduate School of Biomedical Sciences, Japan
[b] Tissue Engineering and Regenerative Therapeutics in Gastrointestinal Surgery, Nagasaki University Graduate School of Biomedical Sciences, Japan
[c] Department of Gastroenterology and Hepatology, Nagasaki University Graduate School of Biomedical Sciences, Japan

ARTICLE INFO

Article history:
Received 6 July 2022
Received in revised form
12 August 2022
Accepted 28 August 2022

Keywords:
Regenerative medicine
Cell sheet technology
Growth factors
Gastrointestinal tract

ABSTRACT

Introduction: Cell sheet technology has been applied in the treatment of patients with severe cardiac failure. Although the paracrine effect of cell sheets accelerating angiogenesis is thought to be the intrinsic mechanism for improvement of cardiac function, little is known about how a cell sheet would function in the abdomen.

Methods: We used acetic acid-induced gastric ulcer rat model to elucidate the mechanisms of myoblast sheet transplantation in the abdomen. Myoblast sheet was implanted onto the serosal side of the gastric ulcer and the effect of sheet transplantation was analyzed. The maximal diameter of the ulcer and the changes in the gene expression of various growth factors in transplanted site was analyzed. The progenitor marker CD34 was also examined by immunohistochemistry.

Results: Cell sheet transplantation accelerated the ulcer healing. qPCR showed that angiogenic growth factors were significantly upregulated around the ulcer in the transplantation group. In addition, at first, HIF-1a and SDF-1 continued to increase from 3 h after transplantation to 72 h, then VEGF increased significantly after 24 h with a slight delay. An immunohistochemical analysis showed a statistically significant increase in CD34 positivity in the tissue around the ulcer in the transplantation group.

Conclusion: Myoblast sheet secreted various growth factors and cytokines immediately after transplantation onto the serosal side of artificial ulcer in the abdomen. Autonomous secretion, resulting in the time-dependent and well-orchestrated gene expression of various growth factors, plays a crucial role in the cell sheet function. Cell sheet transplantation is expected to be useful to support angiogenesis of the ischemic area in the abdominal cavity.

1. Introduction

The recent advent of endoscopy has enabled safe endoscopic resection of superficial cancers of the gastrointestinal tract. In particular, endoscopic submucosal dissection (ESD) has been established as a curative modality for superficial gastric and colorectal cancer.

ESD is also a useful procedure for managing superficial duodenal neoplasm, which has seen an increase in the number of encountered cases [1–6]. However, duodenal ESD is known to carry a substantial risk of delayed perforation, even if ESD itself is performed without immediate perforation, and once delayed perforations occur, the consequential peritonitis and retroperitonitis result in a potentially lethal condition [7–10].

The presence of bile and pancreatic juice and duodenal wall thinness are thought to be the main causes of delayed perforation,

* Corresponding author. Tissue Engineering and Regenerative Therapeutics in Gastrointestinal Surgery, Nagasaki University Graduate School of Biomedical Sciences, Sakamoto 1-7-1, Nagasaki, 8528102, Japan. Fax: +81-95-819-7319..
E-mail address: kanetaka@nagasaki-u.ac.jp (K. Kanetaka).
Peer review under responsibility of the Japanese Society for Regenerative Medicine.
# These authors contributed equally to this work.

https://doi.org/10.1016/j.reth.2022.08.008

Abbreviations

ESD	endoscopic submucosal dissection
VEGF	Vascular endothelial growth factor
HGF	Hepatocyte growth factor
PDGF	Platelet-derived growth factor
HIF1	αHypoxia inducible factor α
SDF1	Stromal cell-derived factor 1
TGFβ	Transforming growth factorβ

so closure of the mucosal defect after ESD is recommended for preventing these complications in clinical practice [11–13]. In addition to these physiological features of the duodenum, disturbance of the intravascular flow due to extended muscularis propria with endoscopic air supply during ESD and consequent ischemia at the ESD site might be important factors contributing to delayed perforation [14]. A histological analysis of a porcine duodenal ESD model revealed atrophy of the gland and a ghost-like appearance of the surrounding mucosa at the duodenal ESD site. Therefore, reinforcement of the blood supply to the ischemic area after ESD is also crucial for preventing delayed perforation.

In recent years, cell sheet technology has been studied in various fields of regenerative medicine, and clinical studies using cell sheets have been conducted in a wide range of organs, such as the heart, esophagus, middle ear, articular cartilage, periodontal ligament and cornea [15–22]. Although little is known about how cell sheets function at the transplanted site, the paracrine effect of a cell sheet to accelerate angiogenesis is considered an intrinsic mechanism, and the increased expression of angiogenetic factors, such as Vascular endothelial growth factor (VEGF) and Hepatocyte growth factor (HGF) at transplanted site, was reported in a rat model of heart failure after transplantation of a myoblast sheet [23].

We previously reported that myoblast sheet transplantation with omental coverage prevented delayed perforation after duodenal ESD in a porcine model [24]. In that model, we placed a cell sheet in the abdominal cavity and transplanted it to the serosal side of the ESD site. Although the histopathological findings revealed thickening of the wall of the ESD ulcer, the mechanism behind such tissue regeneration caused by transplantation remained unclear.

In the present study, to elucidate the mechanisms involved in intraabdominal transplantation of a myoblast sheet, we used a rat model of mucosal defect caused by acetic acid-induced gastric ulcer and investigated the changes in gene expression at the transplanted area in the very early phase after cell sheet transplantation.

2. Materials and methods

2.1. Animals

All rats received humane care according to the criteria outlined in *the Guide for the Care and Use of Laboratory Animals* prepared by the National Institute of Health (NIH publication 86–23, revied 1985). Animal experimental procedures were performed in accordance with the Guidelines for Animal Experimentation of Nagasaki University with approval of the Institutional Animal Care and Use Committee (Approval No. 1905281532–2).

Eight-week-old male Wistar rats were purchased from CLEA Japan Co., Ltd (Tokyo, Japan). The rats were maintained in an environment of temperature 22 ± 2 °C and humidity 40%–70%; chow (Oriental Yeast, Tokyo, Japan) and autoclaved water were available *ad libitum* at the Laboratory Animal Center for Biochemical Research at Nagasaki University Graduate School of Biomedical Sciences.

2.1.1. Rat myoblasts culture and cell sheet fabrication

Rat myoblasts L8 cells (American Type Culture Collection, Manassas, VA, USA; Cat. No. 95102434), which are commercially available and established from Wistar rats, were seeded onto temperature-responsive culture 6-well plates (UpCell 6 Multi-well plates; Cellseed, Tokyo, Japan; Cat. No. CS3004) at a density of 2×10^5 cells/well. The cells were cultured in medium consisting of DMEM, high glucose (Thermo Fisher Scientific, Waltham, MA, USA; Cat. No. 11995–065), 10% fetal bovine serum (FBS; Thermo Fisher Scientific; Cat. No. 1606731) and 10 μg/mL Gentamicin (Fujiseiyaku, Tokyo, Japan) at 37 °C and 5% CO_2. The medium was replaced with fresh medium every 48–72 h. After 5 days of culture, confluent myoblasts on temperature-responsive dishes were transferred and left to sit at 20 °C for about 2 h, causing the myoblast sheets to detach spontaneously. The myoblast sheets were then washed 3 times with iced Hank's balanced salt solution containing calcium chloride and magnesium sulfate (HBSS+; Thermo Fisher Scientific; Cat. No. 14025–092) and fixed with fibrin tissue glue (Beriplast; CSL Behring, Malburg, Germany; Cat. No. 731141119).

2.1.2. Gastric ulcer induction and myoblast sheet transplantation

The induction of gastric ulcers in rats was processed with modification of a previously reported method [25]. In brief, rats were anesthetized via inhalation of isoflurane (Isoflu; DS Pharma Animal Health, Osaka, Japan). The abdomen was swabbed with an iodinated solution, and an incision was made along the middle of the abdomen. The stomach was exposed, and both the anterior and posterior walls sides of gastric antrum were clamped together with ring forceps (OD 8 × 10 mm) (Fig. 1A). A total of 100 μL of 40% (v/v) acetic acid solution was injected into the clamped lumen with a 26-gauge needle attached to a 1-mL syringe. The injected acid was removed 30 s later.

In the sheet transplantation group, a myoblast sheet was implanted using a round coverslip onto the serosa side of the anterior wall of the stomach where acid solution had been injected (D 20 mm) (Fig. 1C, D, E). In the control group, the abdomen was immediately closed without myoblast sheet transplantation. The rats were fed normally thereafter. Rats in both groups were sacrificed three and seven days after the induction of gastric ulcer, and the maximal diameter of the ulcers was measured using the image analyzer software program, WinROOF version 6.3 (Mitani, Fukui, Japan).

2.1.3. Sampling

For expression analyses, rats were sacrificed 3, 12, 24 and 72 h after the operation, and their stomachs were collected. Three rats in the control group and seven in the transplantation group were examined at each time point. After the rats were sacrificed, the stomachs were harvested for the evaluation and measurement. A part of each specimen was collected from transplanted site of the stomach using a biopsy punch and stored in RNAlater solution (QIAGEN, Hilden, Germany) for total RNA extraction. All remains were fixed with 4% paraformaldehyde phosphate-buffered solution (PFA; FUJIFILM Wako Pure Chemical, Osaka, Japan; Cat. No. 163–20145) for paraffin embedding.

2.2. Histopathological analyses

Serial sections (5 μm) were cut from the paraffin blocks. Hematoxylin-eosin staining (HE) and immunohistochemistry staining (IHC) were performed. IHC was performed with Dako **Target Retrieval Solution,** Citrate **pH** 6 (10x) (Dako-Agilent

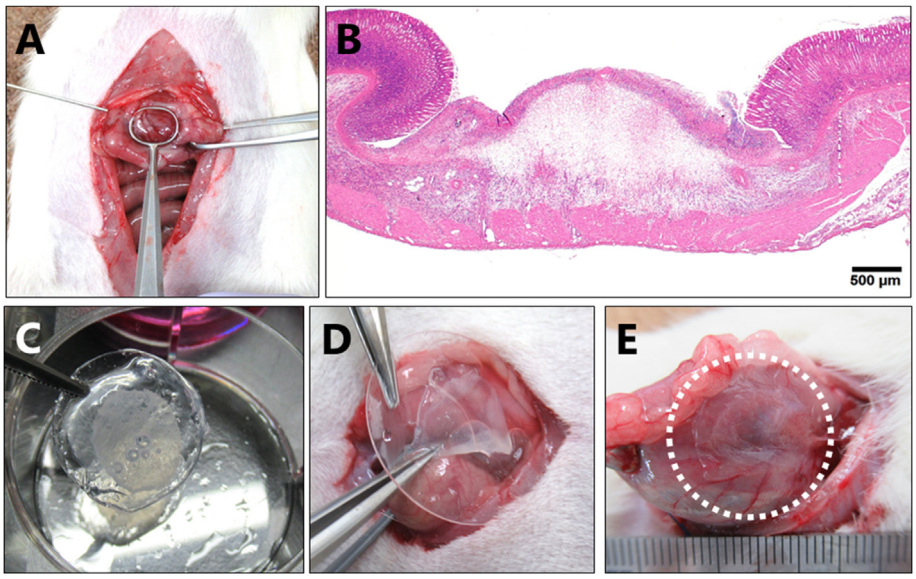

Fig. 1. Development of acetic acid-induced gastric ulcers in rats. A) A total of 100 μL of 40% acetic acid solution was injected into and removed from the clamped lumen using ring forceps with a 26-gauge needle attached to a 1 mL syringe. B) Histopathological findings. The photographs show the acetic acid-induced gastric ulcer on postoperative day (POD) 3. C) A cultured rat myoblast cell sheet was moved onto the round coverslip. D) The cell sheet was transplanted onto the serosa side of the gastric ulcers. E) The transplanted cell sheet is shown in the white dotted circle.

Technologies, Santa Clara, CA, USA; Cat. No. S236784), Dako REAL Peroxidase-Blocking Solution (Cat. No. S2023), Protein Block Serum-Free Ready-to-use (Cat. No. X0909), Dako REAL Antibody Diluent (Cat. No. S2022) and Dako REAL EnVision Detection System, Peroxidase/3,3'-Diaminobenzidine +, Rabbit/Mouse (Cat. No. K5007). These procedures were performed according to Dako's protocol. After visualization with DAB, the sections were counter-stained with hematoxylin. The stained specimens were observed using an Olympus BX53 microscope (Olympus, Tokyo, Japan). The immunopositive areas were measured using WinROOF (Mitani).

The primary antibodies employed were as follows: Rabbit Anti-Desmin antibody (Abcam, Cambridge, UK; Cat. No. ab15200) 1:200, CD34 Monoclonal Antibody (QBEND/10) (Invitrogen-Thermo Fisher Scientific; Cat. No. MA1-10202) 1:500 and Platelet-derived growth factor (PDGF)-A Antibody (E–10: Santa Cruz, Dallas, TX, USA; Cat. No. sc-9974) 1:100.

2.3. Total RNA extraction and quantitative reverse transcription polymerase chain reaction (RT-qPCR)

Total RNA was prepared from the specimens using PureLink RNA Mini Kit (Thermo Fisher Scientific; Cat. No. 12183018 A). The concentration and purity of total RNA were measured using a Thermo Fisher Scientific NanoDrop Lite Spectrophotometer.

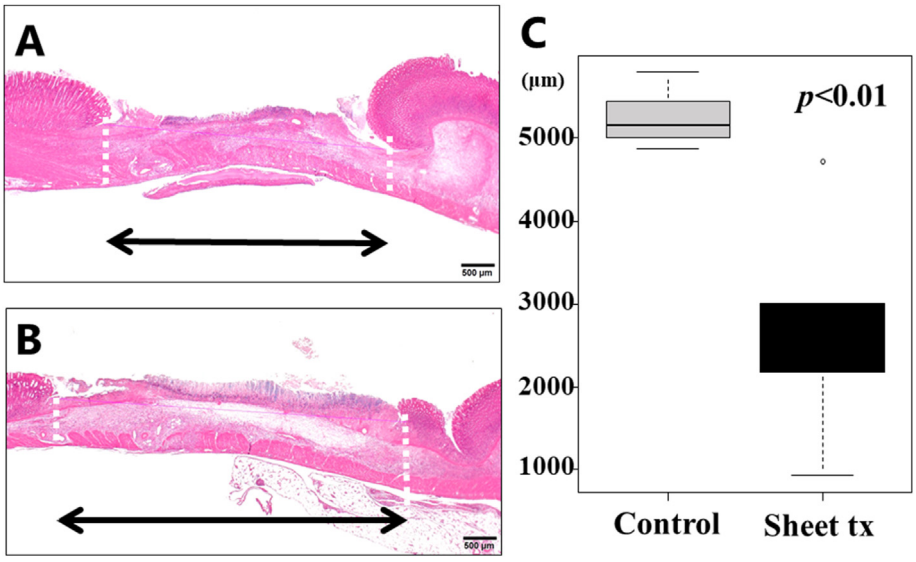

Fig. 2. Comparing the ulcer diameter. Histopathological findings of the ulcer on postoperative day 3 in cell sheet transplantation group (A) and the control group (B). C) The graph shows the ulcer diameter calculated by WinROOF. The box plots represent the minimum, lower quartile, median, upper quartile and maximum, n = 8/5 in biological replicates. The small black circle represent outlier. The p-value according to the Mann–Whitney U-test is indicated (compared with the control group on POD 3).

cDNA was synthesized from 500 ng of total RNA using a High-Capacity cDNA Reverse Transcription Kit (Applied Biosystems-Thermo Fisher Scientific; Cat. No. 4368813). Real-time qPCR was performed using an Applied Biosystems StepOnePlus Real-Time PCR system with TaqMan Fast Advanced Master Mix (Applied Biosystems-Thermo Fisher Scientific; Cat. No. 4444963) and rat-specific TaqMan Gene Expression Assays (FAM). All data were normalized to the 18 S rRNA (Assay ID:Hs99999901_s1) expression. For the relative expression analysis, the ddCT method was used, and the values without cell-sheet transplantation were used as reference values.

The other TaqMan Gene Expression Assays (FAM) employed were as follows: hypoxia inducible factor 1α (Hif1α; Rn 01472831_m1), stromal cell-derived factor 1 (Sdf1; Cxcl12; Rn01462855_m1), vascular endothelial growth factor (Vegf; Rn01511610_m1), transforming growth factor β1 (Tgfβ1; Rn00572010_m1), platelet-derived growth factor-B (Pdgfb; Rn01502597_m1) and chemokine (C-X-C motif) receptor 4 (Cxcr4; Rn01483207_m1).

2.4. Statistical analyses

All samples were obtained by repeated biological examinations which were all carried out three times. Data of quantitative PCR were analyzed by two-tailed Student's *t*-test using the Excel (Microsoft, Redmond, WA, USA). Histopathological data were analyzed by the Mann–Whitney U-test using the EZR Ver. 1.40 (Saitama Medical Center, Jichi Medical University, Saitama, Japan). A p-value of <0.05 was considered statistically significant.

3. Results

3.1. Establishment of an acute mucosal defect rat model

We initially tried to use our original acetic acid-induced gastric ulcer model; however, it was deemed not suitable for elucidating the mechanisms involved in cell sheet transplantation because of the immediate perforation induced by acetic acid injection and consequent severe adhesion around the gastric ulcer at day 3 (data not shown). We had to modify the volume of the injected solution and duration in order to enable observation at least 3 days after injection, and we finally arrived at a model involving injection of 0.1 mL of a 40% acetic acid solution for 30 s that was feasible for our analysis. Under this condition, a histopathological examination confirmed that damage was restricted to the mucosal layer, submucosal layer and lamina propria, and no necrosis or severe inflammation was seen in the proper muscular layer in any of the injected rats from 3 to 72 h after injection. Representative histopathological findings are indicated in Fig. 1B.

3.2. The transplanted myoblast sheet promotes the shrinkage of the ulcer area

Macroscopically, gastric ulcer perforation and abdominal adhesion were not observed in either the control or cell sheet transplantation group three days after initial operation. The myoblast sheet was visible at the transplanted site of the rat stomach in the transplantation group.

In the histopathological examination, the mucosal defect was observed in both groups, and massive infiltration of inflammatory cells was observed around the bottom of the ulcerated area; however, neither gastric wall perforation nor thinning of the muscular layer was noted in either group. We checked the maximal diameter of the ulcers three and seven days after injection using a WinROOF image analyzer to evaluate the effect of cell sheet transplantation. Three days after injection, the diameter of the artificial ulcers in the transplantation group (Fig. 2A) was significantly smaller than in the control group (Fig. 2B and C), although the diameter was identical between the groups at seven days after injection (data not shown). These results suggested that the myoblast sheet promoted the shrinkage of the ulcer area, especially in the early phase of ulcer healing.

3.2.1. High expression of HIF1α, SDF1 and VEGF in the myoblast sheet

The qPCR results showed that various growth factors were significantly upregulated around the ulcer in the transplantation group compared to the control group at various time points in the early phase after transplantation. In addition, different time-dependent patterns of the expression of each growth factor were seen (Fig. 3). The expression of Hypoxia inducible factor1α (HIF1α), Stromal cell-derived factor 1 (SDF1) and Transforming growth factorβ (TGFβ) was upregulated as early as 3 h after transplantation, and this high expression was maintained throughout the examination period. In contrast, the expression of VEGF in the transplantation group was almost identical to that in the control group immediately after the operation but peaked at 24 h after transplantation. The expression of CXCR4, a known SDF1 receptor, was also increased in the late phase of the examination period.

3.2.2. CD34-positive cells were increased around the myoblast sheet transplantation area

As VEGF and TGFβ upregulation is known to play a central role in angiogenesis, we explored the expression of the endothelial progenitor cell marker CD34 in an immunohistochemical analysis. Statistically significant increases in CD34 positivity were shown in the tissue around the artificial ulcer in the transplantation group (Fig. 4A and B) compared to the control group (Fig. 4C and D) at three days after injection. Fig. 4E shows the box plots of the ratio of the immunopositive area calculated by the WinROOF.

Similarly, we also checked the expression of the bone marrow-mesenchymal stem cell (B-MSC) marker PDGF-A. The result suggested that PDGF-A-positive cells were more prolific in the transplantation group (Fig. 5A and B) than in the control group (Fig. 5C and D), although the difference was not statistically significant (Fig. 5E).

To explore whether the origins of these CD34-and PDGF-A-positive cells are transplanted cells or not, we rechecked the positivity of immunohistochemically-stained cell sheets before and after transplantation under magnified views. Before transplantation, the cell sheet was negative for CD34 and these cells were also negative after transplantation (Fig. 6A and B). This indicated that CD34-positive cells detected in the whole gastric wall were not derived from the transplanted cells. In contrast, the cell sheet was positive for PDGF-A both before and after transplantation (Fig. 6C and D).

4. Discussion

Our present data demonstrated that intraabdominally transplanted cell sheet autonomously secreted various growth factors immediately after transplantation in a time-dependent and well-orchestrated manner, which contributed to the promotion of healing of the artificial ulcer.

We recently reported the efficacy of cell sheet transplantation on preventing delayed perforation after duodenal ESD when transplanted onto the serosal side in porcine abdomen [24]. To elucidate the mechanism by which cell sheets prevent delayed perforation after duodenal ESD, we used an acetate injection-induced ulcer rat model instead of a porcine ESD model because

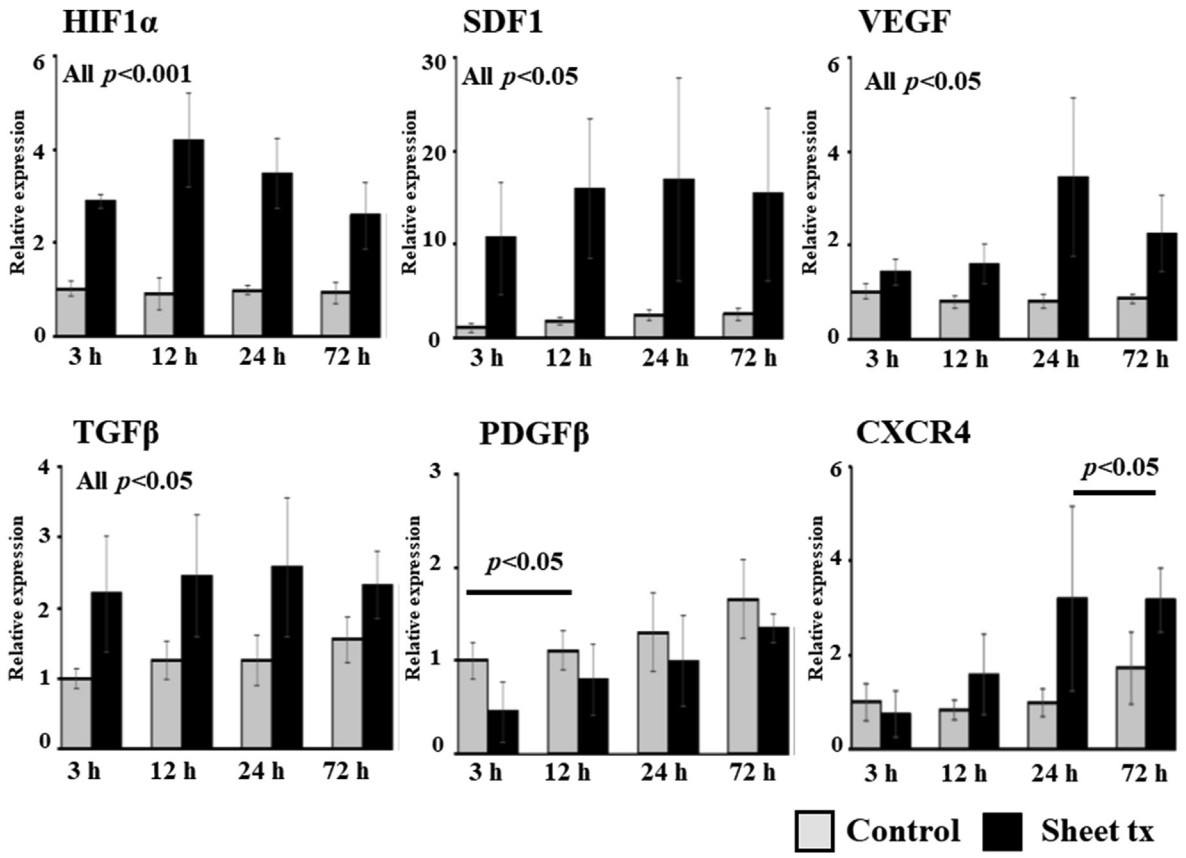

Fig. 3. Gene expression profile in the ulcer area by RT-qPCR. These graphs show the relative expression in the area of the ulcer in the sheet transplantation group relative to that in the control group. All gene levels were normalized to 18 S rRNA. Error bars represent mean ± SD, n = 5 in biological replicates. The p-value according to the two-tailed Student's *t*-test is indicated in comparison with the expression in the control group 3 h after acetate injection.

with this model it was technically easier to perform both molecular and histochemical analyses.

We first determined the appropriate injection volume and exposure duration to allow observation for at least three days after the induction of artificial ulcer. Our data in this model indicated that cell sheet transplantation accelerated the healing process of ulceration, since the maximal diameter of the ulcer was smaller in the transplantation group than in the control group. This result convinced us that this rat artificial ulcer model could replicate our ESD porcine model, allowing us to conduct further analyses using this model to explore the mechanism behind the prevention of delayed perforation after cell sheet transplantation.

A gene expression analysis at the transplanted site showed that mRNA of various growth factors, such as HIF1α, SDF1 and VEGF, was expressed in the very early phase after transplantation. Memon et al. also reported that various growth factors were secreted from a myoblast sheet transplanted onto a heart [23]. They found that these growth factors accelerated angiogenesis and increased the blood supply at the transplanted site, leading to improvement in the cardiac function. Furthermore, Kainuma et al. reported that accompanied transplantation of pedicled omentum with a cell sheet showed improvement of donor cell retention and more stable angiogenesis than single treatment with either a cell sheet or omentum alone in acute myocardial ischemic rat model [26]. They speculated that this synergistic effect was due to the upregulated expression of both VEGF and SDF1 and suggested that these growth factors and cytokines stimulate migration of endothelial cells from both the host myocardium and the omentum toward the sheet, establishing robust vessel connections between native artery and omentum and resulting in improved microcirculation.

Recently, we revealed that a crucial cause of delayed perforation after duodenal ESD is ischemic changes around the mucosal defect [14], and cell sheet transplantation with omental coverage can promote tissue regeneration to prevent this lethal complication [24]. While we were unable to evaluate the gene expression profile in our porcine ESD model, the data obtained in our rats strongly suggest that revascularization at the ischemic area from the omentum and improvement of blood flow by cell sheet transplantation play a crucial role in tissue regeneration at the ESD site.

In addition, our results showed that growth factors, such as TGFβ and VEGF, were secreted in a time-dependent and well-orchestrated manner immediately after transplantation. Anderson et al. emphasized that the combination of several growth factors is important for the maturation of endothelial cells [27]. Siltanen et al. also indicated that transplantation of myoblast sheets highly producing a single paracrine mediator, HGF, was not sufficient to improve the cardiac function in models of acute and chronic heart failure [28]. This indicated that the timing and order of the secretion of various soluble factors might be more important for ensuring effective cell sheet transplantation than hyperexpression of a single gene.

Omentum also has the potential to supply fat-derived stem cells and progenitor cells, which also contribute to new vessel growth and tissue regeneration [27,29,30]. We demonstrated that SDF1 was expressed in the very early phase of myoblast sheet transplantation. SDF1 plays a crucial role in the recruitment of various stem and progenitor cells from peripheral blood to induce neovascularization through its receptor CXCR4, which is widely expressed on endothelial progenitor cells [31,32]. In addition, the SDF1/CXCR4 axis has been well documented to play a significant

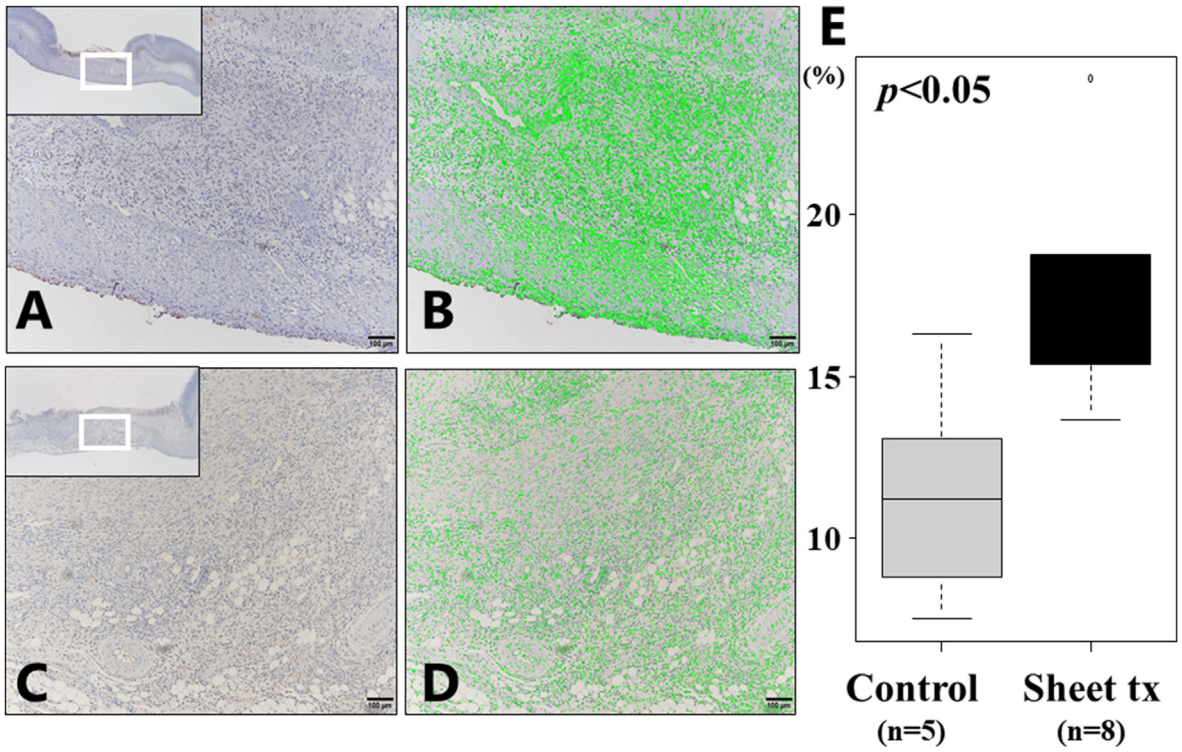

Fig. 4. Comparing CD34-positive cell numbers in the ulcer areas. Immuno-histochemical staining was performed using anti-CD34 antibodies. The photographs show CD34-positive cells as a brown area in cell sheet transplantation group (A) and the control group (C). The middle photographs show WinROOF digital images, with green corresponding to the area of CD34-positive cells in cell sheet transplantation group (B) and the control group (D). E) The box plots showed the ratio of the immunopositive area calculated by WinROOF. The box plots represent the minimum, lower quartile, median, upper quartile and maximum in biological replicates. The small black circle represent outlier. The p-value according to the Mann–Whitney U-test is indicated in comparison with the control group on postoperative day 3.

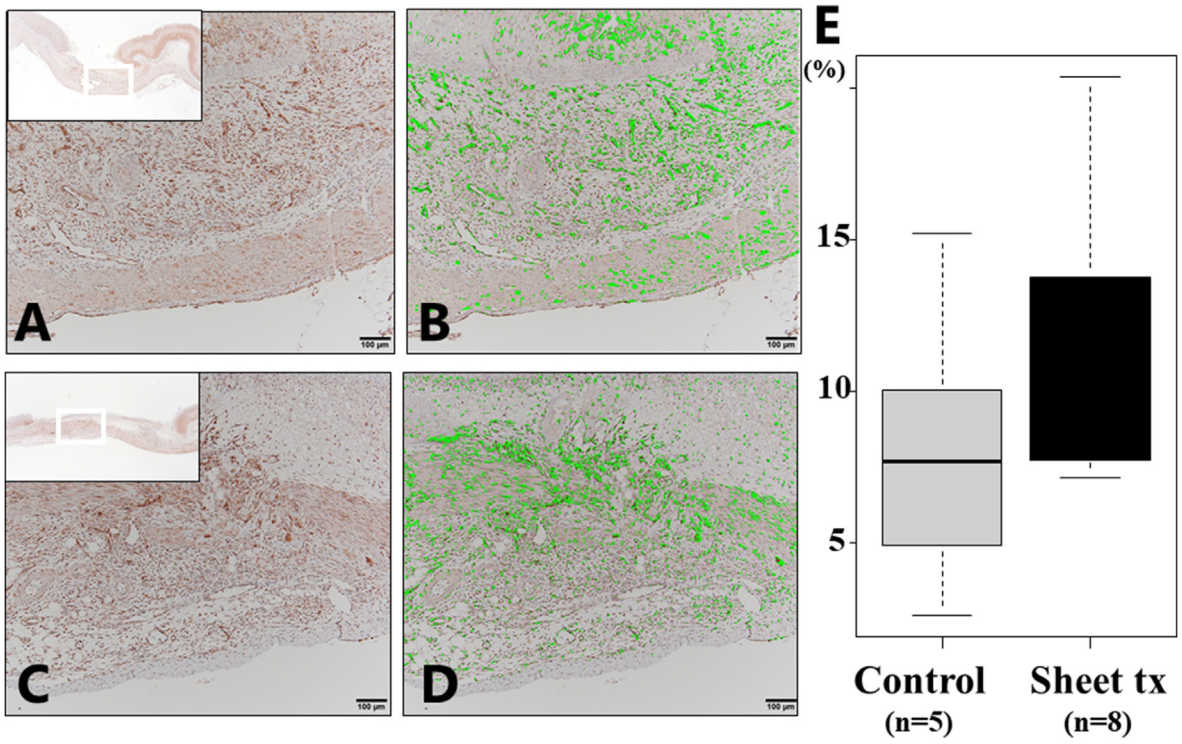

Fig. 5. Comparing PDGF-A-positive cell numbers in the ulcer areas. A) Immuno-histochemical staining was performed using anti-PDGF-A-antibody. The photographs show PDGF-A positive cells as a brown area in cell sheet transplantation group (A) and the control group (C). The middle photographs showed WinROOF digital images, with green corresponding to the area of PDGF-A-positive cells in cell sheet transplantation group (B) and the control group (D). E) The box plots show the ratio of the immunopositive area calculated by WinROOF. The box plots represent the minimum, lower quartile, median, upper quartile and maximum in biological replicates.

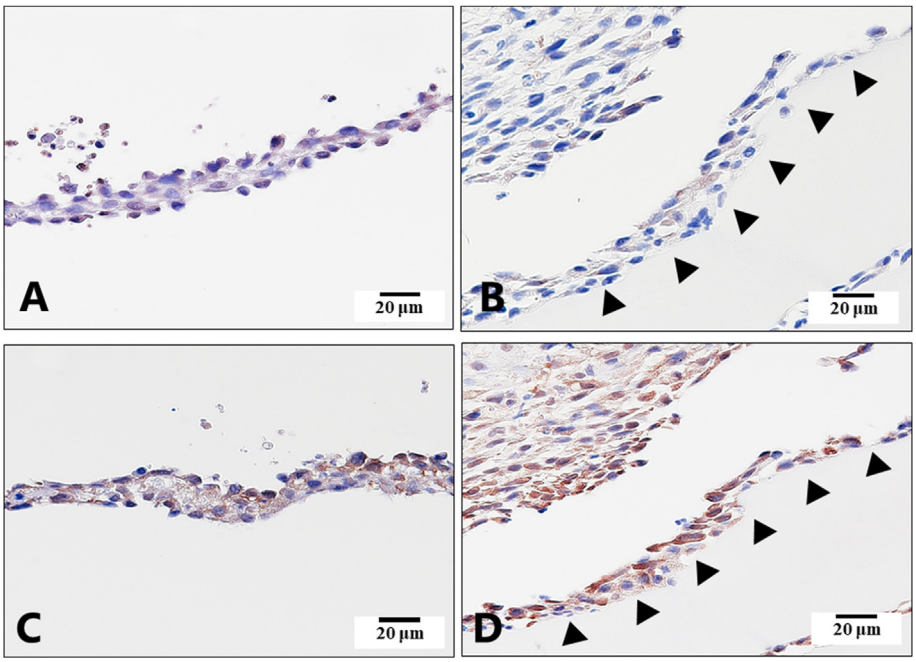

Fig. 6. Histopathological findings of Rat myoblast L8 cell sheet in *vitro/vivo*. Immuno-histochemical staining was performed using anti-CD34 (A and B) and the anti-PDGF-A (C and D) antibodies. The left photographs show myoblast sheet before transplantation. The right photographs show myoblast sheet on postoperative day 3. The arrows in photographs (B) and (D) show myoblast-like cells that were supported by residual fibrin glue on the surface of the transplanted site.

role in the recruitment of hematopoietic stem cells from the bone marrow [33]. Our data implied that the SDF1/CXCR4 axis might also function in the recruitment of endothelial cells from omentum, although we only detected a statistically significant increase in the expression of the CXCR gene between the sheet transplantation and control group in the late phase. SDF1 is involved in the mobilization of progenitor cells to wound sites and facilitation of repair [32,34], and CD34 is regarded as a marker of these hematopoietic and several hematopoietic stem cells including endothelial progenitors [35]. We found that CD34-positive cells were more abundant around the ulceration site in the transplantation group than in the control group according to immunohistochemistry. This finding was also noted by Memon et al. who reported that markedly higher numbers of CD34-positive cells were observed in the group with myoblast sheet transplantation at the infarcted myocardial wall [23].

CD34 was not detected in the cell sheet before transplantation or in the sheet transplanted on the serosal side of the gastric wall. These findings indicated that the origin of these CD34-positive cells may not be transplanted cells themselves but various native cells, such as inflammatory cells and hematopoietic stem cells. In contrast, PDGF-A was positive in cell sheets both before and after transplantation. Although PDGF is known as a bone marrow-mesenchymal stem cell marker, a possible role in myoblast proliferation has been reported [36]. PDGF-A positivity of a cell sheet may reflect cellular proliferation.

Several limitations associated with the present study warrant mention. We used a small animal model instead of a porcine model to elucidate the mechanisms involved in cell sheet transplantation because an expression analysis is easy in such a model due to the availability of primers. The healing process of the mucosal defect might differ between the porcine model, which used electric device cutting, and the acetate-induced ulcer rat model, which used chemical ablation. We were also unable to exclude instances of immunoreaction around the cell sheet in transplanted site. We used autologous myoblasts obtained from the femur in recipient pigs, whereas we used commercially available established myoblasts to fabricate a myoblast sheet in the rat model. Although these myoblasts were derived from the same strain of rat, they were not purely autologous.

In conclusion, the present study revealed that the transplanted myoblast sheet secreted various growth factors and cytokines immediately after abdominal transplantation. Autonomous secretion, resulting in the time-dependent and well-orchestrated expression of various growth factors, plays a crucial role in the cell sheet function. Cell sheet transplantation is therefore expected to be useful for not only improving the cardiac function, but also to support angiogenesis of the ischemic area in the abdominal cavity.

Author contributions

Conceptualization: Kengo Kanetaka
Methodology: Shinichiro Kobayashi, Yasuhiro Maruya, Hashiguchi Keiichi
Writing-original draft preparation: Miki Higashi, Shun Yamaguchi
Writing-review and editing: Kengo Kanetaka, Masaaki Hidaka
Surpervision: Susumu Eguchi, Kazuhiko Nakao

Declaration of competing interest

Drs. Yamaguchi, Kobayashi, Hashiguchi, Nakao and Eguchi have no conflicts of interest or financial ties to disclose. The laboratory which Drs. Higashi, Kanetaka and Maruya belong to received funding for cooperative research in cell sheet from the TERUMO company.

Acknowledgments

We thank Ms. Hideko Hasegawa for helpful discussions and technical support.

This research was supported by Japan Agency for Medical Research and Development (AMED) under Grant Number JP20bk0104112h0001 (Kengo Kanetaka). Also, this research was partially supported by Japan Society for the Promotion of Science (JSPS) KAKENHI Grant Number JP18K16368 (Yasuhiro Maruya.).

References

[1] Schottenfeld D, Beebe-Dimmer JL, Vigneau FD. The epidemiology and pathogenesis of neoplasia in the small intestine. Ann Epidemiol 2009;19:58–69.
[2] Lu Y, Frobom R, Lagergren J. Incidence patterns of small bowel cancer in a population-based study in Sweden: increase in duodenal adenocarcinoma. Cancer Epidemiol 2012;36:e158–63.
[3] Goda K, Kikuchi D, Yamamoto Y, Takimoto K, Kakushima N, Morita Y, et al. Endoscopic diagnosis of superficial non-ampullary duodenal epithelial tumors in Japan: multicenter case series. Dig Endosc 2014;26(Suppl 2):23–9.
[4] Legue LM, Bernards N, Gerritse SL, van Oudheusden TR, de Hingh IH, Creemers GM, et al. Trends in incidence, treatment and survival of small bowel adenocarcinomas between 1999 and 2013: a population-based study in The Netherlands. Acta Oncol 2016;55:1183–9.
[5] Kakushima N, Yoshida M, Yabuuchi Y, Kawata N, Takizawa K, Kishida Y, et al. Present status of endoscopic submucosal dissection for non-ampullary duodenal epithelial tumors. Clin Endosc 2020;53:652–8.
[6] Yoshida M, Yabuuchi Y, Kakushima N, Kato M, Iguchi M, Yamamoto Y, et al. The incidence of non-ampullary duodenal cancer in Japan: the first analysis of a national cancer registry. J Gastroenterol Hepatol 2021;36:1216–21.
[7] Inoue T, Uedo N, Yamashina T, Yamamoto S, Hanaoka N, Takeuchi Y, et al. Delayed perforation: a hazardous complication of endoscopic resection for non-ampullary duodenal neoplasm. Dig Endosc 2014;26:220–7.
[8] Nonaka S, Oda I, Tada K, Mori G, Sato Y, Abe S, et al. Clinical outcome of endoscopic resection for nonampullary duodenal tumors. Endoscopy 2015;47:129–35.
[9] Yahagi N, Kato M, Ochiai Y, Maehata T, Sasaki M, Kiguchi Y, et al. Outcomes of endoscopic resection for superficial duodenal epithelial neoplasia. Gastrointest Endosc 2018;88:676–82.
[10] Hara Y, Goda K, Dobashi A, Ohya TR, Kato M, Sumiyama K, et al. Short- and long-term outcomes of endoscopically treated superficial non-ampullary duodenal epithelial tumors. World J Gastroenterol 2019;25:707–18.
[11] Kato M, Ochiai Y, Fukuhara S, Maehata T, Sasaki M, Kiguchi Y, et al. Clinical impact of closure of the mucosal defect after duodenal endoscopic submucosal dissection. Gastrointest Endosc 2019;89:87–93.
[12] Tsutsumi K, Kato M, Kakushima N, Iguchi M, Yamamoto Y, Kanetaka K, et al. Efficacy of endoscopic preventive procedures to reduce delayed adverse events after endoscopic resection of superficial nonampullary duodenal epithelial tumors: a meta-analysis of observational comparative trials. Gastrointest Endosc 2021;93:367–374 e3.
[13] Takimoto K, Matsuura N, Nakano Y, Tsuji Y, Takizawa K, Morita Y, et al. Efficacy of polyglycolic acid sheeting with fibrin glue for perforations related to gastrointestinal endoscopic procedures: a multicenter retrospective cohort study. Surg Endosc 2022;36:5084–93.
[14] Hashiguchi K, Maruya Y, Matsumoto R, Yamaguchi S, Ogihara K, Ohnita K, et al. Establishment of an in-vivo porcine delayed perforation model after duodenal endoscopic submucosal dissection. Dig Endosc 2021;33:381–9.
[15] Nishida K, Yamato M, Hayashida Y, Watanabe K, Yamamoto K, Adachi E, et al. Corneal reconstruction with tissue-engineered cell sheets composed of autologous oral mucosal epithelium. N Engl J Med 2004;351:1187–96.
[16] Ohki T, Yamato M, Ota M, Takagi R, Murakami D, Kondo M, et al. Prevention of esophageal stricture after endoscopic submucosal dissection using tissue-engineered cell sheets. Gastroenterology 2012;143:582–588 e2.
[17] Sawa Y, Yoshikawa Y, Toda K, Fukushima S, Yamazaki K, Ono M, et al. Safety and efficacy of autologous skeletal myoblast sheets (TCD-51073) for the treatment of severe chronic heart failure due to ischemic heart disease. Circ J 2015;79:991–9.
[18] Yamamoto K, Yamato M, Morino T, Sugiyama H, Takagi R, Yaguchi Y, et al. Middle ear mucosal regeneration by tissue-engineered cell sheet transplantation. NPJ Regen Med 2017;2:6.
[19] Yamaguchi N, Isomoto H, Kobayashi S, Kanai N, Kanetaka K, Sakai Y, et al. Oral epithelial cell sheets engraftment for esophageal strictures after endoscopic submucosal dissection of squamous cell carcinoma and airplane transportation. Sci Rep 2017;7:17460.
[20] Iwata T, Yamato M, Washio K, Yoshida T, Tsumanuma Y, Yamada A, et al. Periodontal regeneration with autologous periodontal ligament-derived cell sheets - a safety and efficacy study in ten patients. Regen Ther 2018;9:38–44.
[21] Sato M, Yamato M, Mitani G, Takagaki T, Hamahashi K, Nakamura Y, et al. Combined surgery and chondrocyte cell-sheet transplantation improves clinical and structural outcomes in knee osteoarthritis. NPJ Regen Med 2019;4:4.
[22] Kanzaki M, Takagi R, Washio K, Kokubo M, Mitsuboshi S, Isaka T, et al. Bioartificial pleura using autologous dermal fibroblast sheets to mitigate air leaks during thoracoscopic lung resection. NPJ Regen Med 2021;6:2.
[23] Memon IA, Sawa Y, Fukushima N, Matsumiya G, Miyagawa S, Taketani S, et al. Repair of impaired myocardium by means of implantation of engineered autologous myoblast sheets. J Thorac Cardiovasc Surg 2005;130:1333–41.
[24] Matsumoto R, Kanetaka K, Maruya Y, Yamaguchi S, Kobayashi S, Miyamoto D, et al. The efficacy of autologous myoblast sheet transplantation to prevent perforation after duodenal endoscopic submucosal dissection in porcine model. Cell Transplant 2020;29:963689720963882.
[25] Tsukimi Y, Okabe S. Effect of anterior unilateral vagotomy on healing of kissing gastric ulcers induced in rats. Jpn J Pharmacol 1994;66:105–14.
[26] Kainuma S, Miyagawa S, Fukushima S, Pearson J, Chen YC, Saito A, et al. Cell-sheet therapy with omentopexy promotes arteriogenesis and improves coronary circulation physiology in failing heart. Mol Ther 2015;23:374–86.
[27] Anderson EM, Mooney DJ. The combination of vascular endothelial growth factor and stromal cell-derived factor induces superior angiogenic sprouting by outgrowth endothelial cells. J Vasc Res 2015;52:62–9.
[28] Siltanen A, Kitabayashi K, Lakkisto P, Makela J, Patila T, Ono M, et al. hHGF overexpression in myoblast sheets enhances their angiogenic potential in rat chronic heart failure. PLoS One 2011;6:e19161.
[29] Kanamori T, Watanabe G, Yasuda T, Nagamine H, Kamiya H, Koshida Y. Hybrid surgical angiogenesis: omentopexy can enhance myocardial angiogenesis induced by cell therapy. Ann Thorac Surg 2006;81:160–7.
[30] Takaba K, Jiang C, Nemoto S, Saji Y, Ikeda T, Urayama S, et al. A combination of omental flap and growth factor therapy induces arteriogenesis and increases myocardial perfusion in chronic myocardial ischemia: evolving concept of biologic coronary artery bypass grafting. J Thorac Cardiovasc Surg 2006;132:891–9.
[31] Askari AT, Unzek S, Popovic ZB, Goldman CK, Forudi F, Kiedrowski M, et al. Effect of stromal-cell-derived factor 1 on stem-cell homing and tissue regeneration in ischaemic cardiomyopathy. Lancet 2003;362:697–703.
[32] Deshane J, Chen S, Caballero S, Grochot-Przeczek A, Was H, Li Calzi S, et al. Stromal cell-derived factor 1 promotes angiogenesis via a heme oxygenase 1-dependent mechanism. J Exp Med 2007;204:605–18.
[33] Xue F, Bai Y, Jiang Y, Liu J, Jian K. Construction and a preliminary study of paracrine effect of bone marrow-derived endothelial progenitor cell sheet. Cell Tissue Bank 2022;23:185–97.
[34] Kozakowska M, Kotlinowski J, Grochot-Przeczek A, Ciesla M, Pilecki B, Derlacz R, et al. Myoblast-conditioned media improve regeneration and revascularization of ischemic muscles in diabetic mice. Stem Cell Res Ther 2015;6:61.
[35] Sidney LE, Branch MJ, Dunphy SE, Dua HS, Hopkinson A. Concise review: evidence for CD34 as a common marker for diverse progenitors. Stem Cell 2014;32:1380–9.
[36] Jin P, Rahm M, Claesson-Welsh L, Heldin CH, Sejersen T. Expression of PDGF A-chain and beta-receptor genes during rat myoblast differentiation. J Cell Biol 1990;110:1665–72.